IEEE Access
Multidisciplinary | Rapid Review | Open Access Journal

Received September 30, 2020, accepted October 8, 2020, date of publication October 12, 2020, date of current version October 22, 2020.

Digital Object Identifier 10.1109/ACCESS.2020.3030159

An Optimizing Method of OFDM Radar Communication and Jamming Shared Waveform Based on Improved Greedy Algorithm

SHENGKUN ZHU[1], RUIJUAN YANG[1], XIAOBAI LI[1], JIAJUN ZUO[1], DONGJIN LI[1], AND YATING DING[2]

[1]People's Liberation Army, Air Force Early Warning Academy, Wuhan 430000, China
[2]Department of Sociology, Wuhan University, Wuhan 430000, China

Corresponding author: Xiaobai Li (lxb2cici@163.com)

This work was supported in part by the National Defense Science and Technology Innovation Zone Fund of China under Grant 17H86304ZT00302201.

ABSTRACT Orthogonal frequency division multiplexing (OFDM) has been widely used as radar, communication, and jamming shared waveform. To improve the power utilization and efficiency of radar, communication, and jamming integrated system, we propose an adaptive OFDM shared waveform design method. Considering the problem of jamming path propagation loss and sensitivity of frequency response error of radar and communication channels, we propose a robust OFDM shared waveform design method. Firstly, the suppressed jamming entropy model, the detection probability (Pd) of the stationary point target model, the data information rate (DIR) model with a given bit error rate (BER) are formulated. With the constraints on total power and BER, the adaptive and the robust OFDM optimization problems are formulated. Then we derive the Karush-Kuhn-Tucker (KKT) conditions of the two optimization problems and an improved greedy algorithm is proposed to solve the optimization problems, and the optimal power and bit allocation schemes for the two problems are obtained. Finally, we present several numerical results to demonstrate the effectiveness of the proposed method.

INDEX TERMS Orthogonal frequency division multiplexing (OFDM), adaptive OFDM shared waveform design, robust OFDM shared waveform design, suppressed jamming entropy, detection probability, data information rate, improved greedy algorithm.

I. INTRODUCTION

With the development of electronic information technology and the demand for information warfare, the integration of multi-functional electronic systems is an effective way to solve the problem of low comprehensive efficiency of radar, communication, and jamming integrated systems [1]. In recent years, research shows that radar, communication, and jamming can be integrated through the OFDM shared waveform [2]–[4]. This kind of OFDM radar, communication, and jamming shared waveform carries communication data. The receiver extracts communication information through demodulation and extracts target information through radar signal reception processing[5]. Jammingmainly includes suppression jamming and deceptive jamming [6]–[10]. Radar, communication and jamming integrated system can suppress the enemy radar by transmitting the OFDM shared waveform to reduce the signal to a jamming ratio of the enemy radar, and weaken the detection performance and tracking performance of the enemy radar. The optimization design of the adaptive OFDM shared waveform can optimize and adjust the parameters according to the operational demands and channel environment to achieve the optimal efficiency of the integrated system [11].

In the past ten years, considerable attention has been paid to waveform optimization methods of radar, communication, and jamming integration. Liu *et al.* [12] investigates a waveform optimization method to maximize conditional mutual information and channel capacity based on information theory. Research in [13] derives the speed and distance Cramér–Rao Bounds for estimating range and channel capacity model of OFDM radar and communication shared

The associate editor coordinating the review of this manuscript and approving it for publication was Barbara Masini.

waveform. Shi *et al.* [14] proposes a waveform optimization method to reduce the interception probability of OFDM radar with the conditions of mutual information and DIR. It can be seen that in the adaptive waveform design of OFDM shared signal, channel capacity is generally used as the objective function of communication performance optimization. However, the channel capacity is only the theoretical upper bound of DIR. In the actual bit and power allocation, the DIR is affected by factors such as the scale quantization accuracy of the constellation, which cannot achieve the optimal performance [15]. By adjusting the bit and power of different subcarriers, the DIR of OFDM shared signal can be improved. Hence an appropriate bit and power allocation algorithm is needed to improve the DIR performance. In the aspect of radar performance, research in [16] deals with the synthesis of optimized radar waveforms ensuring spectral compatibility with the overlayed licensed electromagnetic radiators. Chen *et al.* [17] proposes a novel approach to optimizing the waveforms of an adaptive distributed MIMO radar. Research in [18] propose a novel waveform design procedure based on constrained maximization of the signal-to-interference ratio and constrained minimization of a suitable correlation index. However, the influence of clutter on target detection performance has not been considered in the current research. How to combine subcarrier power with radar detection performance is still a problem. In terms of the jamming performance, the research on the shared waveform optimization for the suppression jamming is very few. Entropy is a norm to measure the performance of suppressed jamming, hence we need to associate entropy with the bit and power allocation of different subcarriers [6]. In practical application, the jamming path transmission loss and the frequency response of radar and communication channels are very difficult to estimate [19]. How we can get the optimal waveform in the worst cases and optimize the configuration of radar, communication, and jamming integrated waveform remains a problem.

Aiming at the above problems, this paper proposes an adaptive OFDM shared waveform optimization method based on suppression jamming and radar detection performance. At the transmitter, the entropy of the OFDM shared waveform with the path transmission loss is taken as the suppression jamming performance criteria. The detection probability of the point target is taken as the radar performance criteria. The data information rate with the given error rate is taken as the communication performance criteria. The adaptive waveform design model is established based on the three criteria. However, the feedback of environment information may not be accurate in practical application. To solve this problem, we propose a robust OFDM shared signal waveform optimization method under the worst channel characteristics. Then KKT conditions are given based on the adaptive and robust OFDM shared waveform. Finally, an improved greedy algorithm is proposed for power and bit allocation with the weighted optimal criterion. The simulation results show that the performance of this method is close to the theoretically optimal value, and the robust OFDM shared waveform improves the radar, communication, and jamming performance in the worst cases.

The rest of this paper is organized as follows. In section II, the OFDM shared waveform model is established and the suppressed jamming entropy, Pd, and DIR are formulated. The adaptive and robust OFDM shared waveform design methods, and the improved greedy algorithm are proposed in Section III. In Section IV, several numerical simulations are presented. Finally, conclusions and future work are given in Section V.

II. GUIDELINES FOR MANUSCRIPT PREPARATION

A. SIGNAL MODEL

The time-domain OFDM shared waveform $s(t)$ can be described as [20]:

$$\begin{aligned} s_m(t) &= e^{j2\pi f_c t}\sum_{n=1}^{N_s} a_m c_{m,n} e^{j2\pi m\Delta f(t-nT_s)} rect\left[\frac{t-T_s}{T_s}\right] \\ s(t) &= \sum_{m=1}^{N_c} s_m(t) \\ &= e^{j2\pi f_c t}\sum_{n=1}^{N_s}\sum_{m=1}^{N_c} a_m c_{m,n} e^{j2\pi m\Delta f(t-nT_s)} rect\left[\frac{t-T_s}{T_s}\right] \end{aligned} \tag{1}$$

where $s_m(t)$ is the transmission signal model of the m-th subchannel, N_c is the number of the subcarriers, f_c is the subcarriers' center frequency, a_m is the m-th subcarrier's complex weight, $c_{m,n}$ is the communication information modulated by the m-th subcarrier, and the n-th OFDM symbol, $\Delta f = 1/T$, where T is the duration of each OFDM symbol, T_s is the time interval of each OFDM symbol, $T_s = T + T_g$, where T_g is the duration of each cycle prefix, $rect\left[t/T_s\right]$ is a rectangular function, which is equal to one for $0 < t < T_s$, and zero, otherwise.

B. JAMMING WAVEFORM CRITERION

Radar target detection should be carried out in noise, and the hypothesis test of whether there is a target in the received signal is uncertain [21]. Therefore, the best-suppressed jamming waveform is the waveform with the largest uncertainty. The measure of uncertainty of random variables is entropy. For continuous random variables, entropy is defined as

$$H(x) = -\int_{-\infty}^{+\infty} p(x)\log_a p(x)\,dx \tag{2}$$

According to the central limit theorem, the probability density of the OFDM signal tends to normal distribution [22]. When the probability density function is a normal distribution, the entropy S can be simplified as follows:

$$\begin{aligned} S &= \ln\sqrt{2\pi e p_T} \\ p_T &= \sum_{m=1}^{N_c} p_m \end{aligned} \tag{3}$$

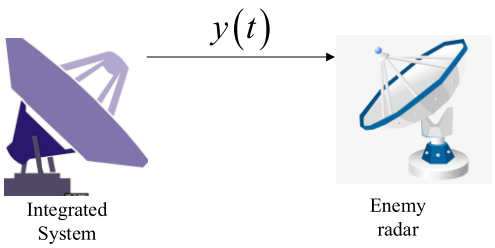

FIGURE 1. Suppression jamming of the OFDM integrated system to enemy radar.

where p_T is transmitting power, p_m is the transmitting power of the m-th subcarrier. In Figure 1, assume that d is the distance between the enemy radar and the OFDM integrated system. The OFDM shared waveform is used to impose a suppressed jamming on the enemy radar. The jamming signal $y(t)$ can be expressed as follows:

$$\begin{aligned} y(t) &= \sum_{m=1}^{N_c} \beta_m s_m(t-\tau) \\ &= e^{j2\pi f_c(t-\tau)} \sum_{n=1}^{N_s} \sum_{m=1}^{N_c} \beta_m a_m c_{m,n} e^{j2\pi m \Delta f(t-\tau-nT_s)} \\ &\quad \times rect\left[\frac{t-\tau-T_s}{T_s}\right] \end{aligned} \tag{4}$$

where τ is the time delay, $\boldsymbol{\beta} = [\beta_1, \beta_2, \ldots, \beta_m], m = 1, 2, \ldots, N_c$ is a response caused by path propagation loss.

Assuming that the modulation data at different positions of OFDM are independent to each other [12], the following equation can be obtained:

$$E\left[a_m a_{m'}^* c_{m,n} c_{m',n'}^*\right] = \begin{cases} |a_m|^2, & m = m', n = n' \\ 0, & \text{else} \end{cases} \tag{5}$$

When the number of subcarriers is large enough (more than 100), the power of the m-th subcarrier of the jamming waveform can be approximately considered as $p'_m = \beta_m^2 |a_m|^2$. Therefore, the entropy model of OFDM shared signal can be expressed as follows:

$$\begin{aligned} S &= \ln \sqrt{2\pi e \sum_{m=1}^{N_c} p'_m} \\ &= \ln \sqrt{2\pi e \sum_{m=1}^{N_c} \beta_m^2 \left|a_m^2\right|} \end{aligned} \tag{6}$$

To improve the ability of suppressed interference of OFDM shared waveform, with the constraint of total power, the waveform design problem of maximizing entropy can be expressed as the problem of maximizing $\sum_{m=1}^{N_c} p'_m$:

$$\begin{aligned} &\max \sum_{m=1}^{N_c} \beta_m^2 |a_m|^2 \\ &s.t. \sum_{m=1}^{N_c} |a_m|^2 = p_T \end{aligned} \tag{7}$$

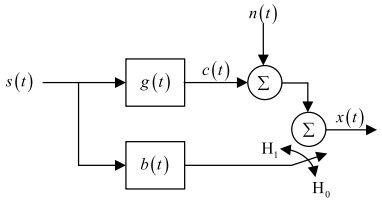

FIGURE 2. Radar received signal model.

The optimization problem in (7) is a linear programming problem, which can be solved by simplex [23]:

$$|a_m|^2 = \begin{cases} p_T & m = \arg\max \beta_m \\ 0 & else \end{cases} \tag{8}$$

It can be seen from (8) that the best jamming waveform is to load all the power on the subcarrier with the best channel conditions. In practical application, this extreme waveform design criterion is not adopted, but it is meaningful to take the result of (8) as the theoretical value.

C. RADAR WAVEFORM CRITERIA

The radar received signal model is shown in Figure 2. The scattering model is assumed to be a random linear time invariant (LTI) filter. Where $x(t) = c(t) + n(t)$, $c(t)$ is clutter echo of the uninterested targets. The clutter can be expressed as the convolution of the transmitted signal and the channel impulse response: $c(t) = s(t) * g(t)$, $g(t)$ is the impulse response of radar channel, which is a generalized stationary random process, mainly reflects the influence of clutter. $n(t)$ is a complex additive white Gaussian noise.

When the false alarm probability is given, the point target detection probability is used as the criteria of radar performance. In the problem of target detection, the observation signal model under two assumptions is as follows:

$$\begin{aligned} H_1 &= As(t) + c(t) + n(t) \\ H_0 &= c(t) + n(t) \end{aligned} \tag{9}$$

Following the guideline in [24], the best detector with the Neyman-Pearson criterion is given:

$$\left| \sum_{m=1}^{N_s} \frac{X(f) S^*(f_m)}{G(f_m) |S(f_m)|^2 + \sigma_r^2(f_m)} \right|^2 > \gamma \tag{10}$$

When (10) is true, the target is judged to exist. Where γ is detection threshold, $X(f)$, $S(f)$ and $G(f)$ are Fourier transform of $x(t)$, $s(t)$ and $g(t)$, $\sigma_r^2(f_m)$ is power spectral density of $n(t)$, $(\cdot)^*$ is a complex conjugate trans-formation, and the detection probability p_d and false alarm probability p_f have the following mathematical relations:

$$\begin{aligned} p_d &= p_{fa}^{\frac{1}{1+\sigma_A^2 d^2}} \\ d^2 &= \sum_{m=1}^{N_s} \frac{|S(f_m)|^2}{G(f_m) |S(f_m)|^2 + \sigma_r^2(f_m)} \end{aligned} \tag{11}$$

where d^2 is the deviation ratio. According to the properties of fourier transform and (1), $|S(f)|^2$ can be obtained as follows:

$$|S(f)|^2 = T_S^2 \sum_{n=0}^{N_s-1}\sum_{m=0}^{N_c-1}\sum_{n'=0}^{N_s-1}\sum_{m'=0}^{N_c-1} a_m a_{m'}^* c_{m,n} c_{m',n'}^* \cdot e^{-j2\pi(f-f_c)(n-n')T_s} e^{-j\pi(m-m')\Delta f T_s} \cdot s_a[\pi(f-f_m)T_s]\cdot s_a[\pi(f-f_{m'})T_s] \quad (12)$$

where $s_a(f) = \sin f / f$. According to (5), $E\left[|S(f)|^2\right]$ can be simplified as follows:

$$E\left[|S(f)|^2\right] = N_s T_s^2 \sum_{m=1}^{N_s} |a_m|^2 s_a^2[\pi(f-f_m)T] \quad (13)$$

When the number of subcarriers is large enough (more than 100), it can be inferred that $|S(f)|^2 \approx E[|S(f)|^2]$. Therefore,

$$|S(f)|^2 \approx N_s T_s^2 \sum_{m=1}^{N_s} |a_m|^2 s_a^2[\pi(f-f_m)T] \quad (14)$$

According to the properties of $s_a(\cdot)$, Equation (14) is reduced to the following equation:

$$|S(f_m)|^2 \approx N_s T_s^2 |a_m|^2 \quad (15)$$

Substituting (15) into (11) yields the expression of d^2 and p_d:

$$p_d = p_{fa}^{\frac{1}{1+\sigma_A^2 d^2}}$$
$$d^2 = \sum_{m=1}^{N_c} \frac{N_s T_s^2 |a_m|^2}{N_s T_s^2 |a_m|^2 G(f_m) + \sigma_r^2(f_m)} \quad (16)$$

To improve the performance of radar point target detection, with the constraint of total power, the problem of maximizing point target detection probability can be simplified as the problem of maximizing deviation ratio d^2:

$$\max d^2 = \sum_{m=1}^{N_c} \frac{N_s T_s^2 |a_m|^2}{N_s T_s^2 |a_m|^2 G(f_m) + \sigma_r^2(f_m)}$$
$$s.t. \sum_{m=1}^{N_c} |a_m|^2 = p_T \quad (17)$$

The optimization problem in (17) is a convex problem [25], which can be solved by the Lagrange multiplier method:

$$|a_m|^2 = \frac{1}{N_s T_s^2}\left[\frac{\sqrt{N_s T_s^2 \sigma_r^2(f_m)/\lambda_m} - \sigma_r^2(f_m)}{G(f_m)}\right]^+ \quad (18)$$

where $[x]^+ = \max\{x, 0\}$, λ_m is Lagrange multiplier, which can be solved by the total power constraint.

D. COMMUNICATION WAVEFORM CRITERIA

In frequency selective fading channel, data information rate (DIR) is often used to measure the communication performance. It is assumed that the communication channel is slow time-varying and frequency-dependent. The communication frequency response $H(f)$ is shown in Figure 3, and its probability density function follows Rayleigh distribution.

The model of DIR in additive white noise channel is as follows:

$$C_t = \sum_{m=1}^{N_c} \Delta f \log_2\left(1 + \frac{|a_m|^2 |H(f_m)|^2}{\Gamma \sigma_c^2}\right) = \sum_{m=1}^{N_c} \Delta f \log_2\left(1 + \frac{p_m |H(f_m)|^2}{\Gamma \sigma_c^2}\right)$$
$$\Gamma = -\frac{\ln(5 \times BER)}{1.5} \quad (19)$$

where p_m is the transmitting power of the m-th subcarrier, $H(f_m)$ is the frequency response of the m-th subcarrier, σ_c^2 is the noise power in the channel, Γ is SNR loss factor [26].

To improve the reliability and effectiveness of OFDM shared waveform, the problem of maximizing DIR with the constraints of power and BER can be expressed as follows:

$$\max\ c = \sum_{m=1}^{N_c} \Delta f \log_2\left(1 + \frac{|a_m|^2 |H(f_m)|^2}{\Gamma \sigma_c^2}\right)$$
$$s.t. \sum_{m=1}^{N_c} |a_m|^2 = p_T \quad (20)$$

The optimization problem in (20) is convex problem. The closed-form solution of the problem can be obtained by the Lagrange multiplier method [27]:

$$|a_m|^2 = \left[\lambda_m - \frac{\Gamma \sigma_c^2}{|H(f_m)|^2}\right]^+ \quad (21)$$

where $[x]^+ = \max\{x, 0\}$, λ_m is Lagrange multiplier, which can be solved by the total power constraint.

III. OPTIMAL DESIGN OF OFDM SHARED WAVEFORM

A. ADAPTIVE OFDM WAVEFORM DESIGN

$$\max F = \frac{\omega_1}{F_1}\sum_{m=1}^{N_c} \beta_m^2 |a_m|^2 + \frac{\omega_2}{F_2}\sum_{m=1}^{N_c} \frac{N_s T_s^2 |a_m|^2}{N_s T_s^2 |a_m|^2 G(f_m) + \sigma_r^2(f_m)} + \frac{\omega_3}{F_3}\sum_{m=1}^{N_c} \log_2\left(1 + \frac{|a_m|^2 |H(f_m)|^2}{\Gamma \sigma_c^2}\right)$$
$$s.t. \begin{cases} \sum_{m=1}^{N_c} |a_m|^2 = p_T \\ |a_m|^2 > 0 \end{cases} \quad (22)$$

where F_1, F_2 and F_3 are the maximum of (7), (17), and (20), ω_1, ω_2 and ω_3 are weighting factors of jamming, radar, and communication's objective functions. $\omega_1 + \omega_2 + \omega_3 = 1$. The problem in (22) is a convex problem, which can be solved by the Karush-Kuhn-Tucker (KKT) condition. The

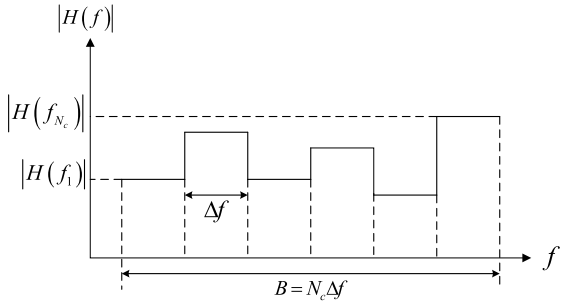

FIGURE 3. Communication frequency response.

KKT condition can be described as

$$\begin{aligned}\mu-\mu_m=&\frac{\omega_1}{F_1}\beta_m^2\left|a_m\right|^2\\&+\frac{\omega_2}{F_2}\frac{N_sT_s^2\sigma_r^2(f_m)}{\left[N_sT_s^2\left|a_m\right|^2G(f_m)+\sigma_r^2(f_m)\right]^2}\\&+\frac{\omega_3}{F_3\ln 2}\frac{\left|H(f_m)\right|^2}{\Gamma\sigma_c^2+\left|a_m\right|^2\left|H(f_m)\right|^2}\\&\mu\left(\sum_{m=1}^{N_c}\left|a_m\right|^2-p_T\right)=0\\&\mu_m\left|a_m\right|^2=0\\&\mu\geq 0,\mu_m\geq 0,\quad m=1,2,...N_c\end{aligned}\tag{23}$$

where μ and μ_m are Lagrange multipliers. The optimal solution of the integrated target function of the adaptive OFDM shared waveform can be obtained by solving (23).

B. ROBUST OFDM WAVEFORM DESIGN

In the last section, the design method of the adaptive OFDM shared waveform is described, but the method needs to know the propagation loss of the jamming path, frequency response of radar channel and frequency response of communication channel, which needs to be obtained by estimation in practical application. When there is an error between the estimated value and the real value, the designed waveform performance is significantly lower than the theoretical performance, and it is difficult to obtain the prior information such as the propagation loss of the jamming path and the frequency response of radar and communication channel. To solve this problem, a robust OFDM shared waveform optimization method is proposed. It is assumed that the path propagation loss and the frequency response of radar and communication channels are in uncertainly class with known upper and lower bounds.

$$\begin{aligned}\Phi_\beta&=\left\{\psi_\beta:0<l_{\beta,m}\leq\psi_{\beta,m}\leq u_{\beta,m},\forall m=1,2,\ldots,N_c\right\}\\\Phi_g&=\left\{\psi_g:0<l_{g,m}\leq\psi_g(f_m)\leq u_{g,m},\forall m=1,2,\ldots,N_c\right\}\\\Phi_h&=\left\{\psi_h:0<l_{h,m}\leq\psi_h(f_m)\leq u_{h,m},\forall m=1,2,\ldots,N_c\right\}\end{aligned}\tag{24}$$

where $\psi_{\beta,m}=\beta_m$, $\psi_g(f_m)=1/G(f_m)$, $\psi_h(f_m)=H(f_m)$, $l_{\beta,m}$ and $u_{\beta,m}$ are the lower and upper bounds of $\psi_{\beta,m}$, $l_{g,m}$ and $u_{g,m}$ are the lower and upper bounds of $\psi_g(f_m)$, $l_{h,m}$ and $u_{h,m}$ are the lower and upper bounds of $\psi_h(f_m)$. Given the upper and lower bounds, according to the minimax criterion, the robust waveform design problem of OFDM shared signal can be described as follows:

$$\begin{aligned}&\max\left\{\min I\left(\boldsymbol{p},\psi_\beta,\psi_g,\psi_h\right)\big|_{1_{N_c}^T\boldsymbol{p}=p_T}\right\}\\&I\left(\boldsymbol{p},\psi_\beta,\psi_g,\psi_h\right)=\frac{\omega_1}{F_1}\sum_{m=1}^{N_c}\psi_{\beta,m}^2\left|a_m\right|^2\\&+\frac{\omega_2}{F_2}\sum_{m=1}^{N_c}\frac{N_sT_s^2\left|a_m\right|^2}{N_sT_s^2\left|a_m\right|^2\psi_g(f_m)+\sigma_r^2(f_m)}\\&+\frac{\omega_3}{F_3}\sum_{m=1}^{N_c}\log_2\left(1+\frac{\left|a_m\right|^2\left|\psi_h(f_m)\right|^2}{\Gamma\sigma_c^2}\right)\end{aligned}\tag{25}$$

where $\boldsymbol{p}=\left[\left|a_1\right|^2,\left|a_2\right|^2,\ldots,\left|a_{N_c}\right|^2\right]$, $I\left(\boldsymbol{p},\psi_\beta,\psi_g,\psi_h\right)$ is the weighting objective function for robust OFDM shared waveform. F_1, F_2 and F_3 are the optimal values of (7), (17) and (20) when path propagation loss and radar and communication frequency response being their upper bounds.

Since $I\left(\boldsymbol{p},\psi_\beta,\psi_g,\psi_h\right)$ is monotonically increasing in $\psi_{\beta,m}$, $\psi_h(f_m)$, and $\psi_g(f_m)$, the minimum value of $I\left(\boldsymbol{p},\psi_\beta,\psi_g,\psi_h\right)$ for $l_{\beta,m}\in\Phi_\beta$, $l_{g,m}\in\Phi_g$, and $l_{h,m}\in\Phi_h$ is $I\left(\boldsymbol{p},l_{\beta,m},l_{g,m},l_{h,m}\right)$, i.e.,

$$\begin{aligned}&\max\left\{\min I\left(\boldsymbol{p},\psi_\beta,\psi_g,\psi_h\right)\big|_{1_{N_c}^T\boldsymbol{p}=p_T}\right\}\\&=\max\left\{I\left(\boldsymbol{p},l_{\beta,m},l_{g,m},l_{h,m}\right)\big|_{1_{N_c}^T\boldsymbol{p}=p_T}\right\}\\&I\left(\boldsymbol{p},l_{\beta,m},l_{g,m},l_{h,m}\right)=\frac{\omega_1}{F_1}\sum_{m=1}^{N_c}l_{\beta,m}^2\left|a_m\right|^2\\&+\frac{\omega_2}{F_2}\sum_{m=1}^{N_c}\frac{N_sT_s^2\left|a_m\right|^2}{N_sT_s^2\left|a_m\right|^2/l_{g,m}+\sigma_r^2(f_m)}\\&+\frac{\omega_3}{F_3}\sum_{m=1}^{N_c}\log_2\left(1+\frac{\left|a_m\right|^2\left|l_{h,m}\right|^2}{\Gamma\sigma_c^2}\right)\end{aligned}\tag{26}$$

The problem in (26) is a convex optimization problem, which can be solved by the KKT condition. The KKT condition can be described as

$$\begin{aligned}\mu-\mu_m=&\frac{\omega_1}{F_1}l_{\beta,m}^2\left|a_m\right|^2\\&+\frac{\omega_2}{F_2}\frac{N_sT_s^2\sigma_r^2(f_m)}{\left[N_sT_s^2\left|a_m\right|^2/l_{g,m}+\sigma_r^2(f_m)\right]^2}\\&+\frac{\omega_3}{F_3\ln 2}\frac{\left|l_{h,m}\right|^2}{\Gamma\sigma_c^2+\left|a_m\right|^2\left|l_{h,m}\right|^2}\\&\mu\left(\sum_{m=1}^{N_c}\left|a_m\right|^2-p_T\right)=0\\&\mu_m\left|a_m\right|^2=0\\&\mu\geq 0,\mu_m\geq 0,\quad m=1,2,...N_c\end{aligned}\tag{27}$$

where μ and μ_m are Lagrange multipliers. The optimal solution of the integrated target function of the robust OFDM shared waveform can be obtained by solving (27).

C. BIT AND POWER ALLOCATION METHOD BASED ON IMPROVED GREEDY ALGORITHM

In the practical application of the OFDM integrated system, we should consider not only channels quality but also the bit error performance. Therefore, under different modulation modes, the actual optimal value cannot reach the theoretical optimal value in (23). The basic idea of the greedy algorithm is to sort and search all subcarriers that need the least power to increase one bit, and then add the number of bit allocation of this subcarrier to one [28]. The power constraint in this paper is equality constraint, and the objective function is a multi-objective function, so the greedy algorithm is no longer applicable. Therefore, this paper proposes an improved greedy algorithm to solve the bit and power allocation problem in the practical application of the OFDM integrated system. The idea is to sort out and search out the subcarrier whose target function increases the maximum by one bit, and then add one bit to the bit allocation number of this subcarrier. The algorithm steps are as follows:

STEP 1: Initialize parameters. The initial bit b_m, power p_m, target function value F_m and ratio δ_m allocated by each subcarrier are set to zero, i.e.,

$$b_m = 0, p_m = 0, F_m = 0, \delta_m = 0, \quad m = 1, 2, \ldots, N_c \tag{28}$$

STEP 2: Calculate the total power $\sum_{m=1}^{N_c} p_m$, when $\sum_{m=1}^{N_c} p_m > p_T$, the algorithm is terminated. Then we subtract the overflowing power from the subcarrier which is allocated power at the last time.

STEP 3: Calculate the increased power p'_m, the increased target function value F'_m, and the ratio $\delta_m = \frac{F'_m - F_m}{p'_m - p_m}$ when adding one bit to the m-th subcarrier. $f(b_m)$ is the power when sending one bit with MPSK modulation ($BER = p_e$) [29]:

$$f(b_m) = \begin{cases} 0 & b_m = 0 \\ \frac{\sigma_c^2}{2}\left[Q^{-1}(p_e)\right]^2 & b_m = 1 \\ \frac{\sigma_c^2}{2}\left[Q^{-1}\left(1-\sqrt{1-p_e}\right)\right]^2 & b_m = 2 \\ \frac{\sigma_c^2}{2}\left[\frac{Q^{-1}(p_e/2)}{\sin\left(\pi/2^{b_i}\right)}\right]^2 & b_m \geq 3 \end{cases} \tag{29}$$

$$p'_m = \frac{f(b_m+1) - f(b_m)}{|H(f_m)|^2} \tag{30}$$

$$\begin{aligned} F'_m = {} & \frac{\omega_1}{F_1}\beta_m^2 p'_m \\ & + \frac{\omega_2}{F_2}\frac{N_s T_s^2 p'_m}{N_s T_s^2 p'_m G(f_m) + \sigma_r^2(f_m)} \\ & + \frac{\omega_3}{F_3}\log_2\left(1 + \frac{p'_m |H(f_m)|^2}{\Gamma\sigma_c^2}\right) \end{aligned} \tag{31}$$

$$\delta_m = \frac{F'_m - F_m}{p'_m - p_m} \tag{32}$$

TABLE 1. Time complexity.

Algorithm	Time Complexity
Improved Greedy Algorithm	$O(BN_c)$
Optimal Algorithm	$O(N_c)$

TABLE 2. Simulation parameters.

Parameter	Value
N_c	128
N_s	10
T_g	$1\mu s$
Δf	$0.25MHz$
BER	10^{-5}

STEP 4: Find the maximum value of all subcarriers and the corresponding number *index_max*. Select one randomly when there are multiple maximum values,.

STEP 5: Allocate 1 bit and corresponding power to the subcarrier whose number is *index_max*. Let $m = index\_max$, $b_m = b_m + 1$, $p_m = p'_m$, $F_m = F'_m$. Back to ***STEP 2***.

When QAM modulation is adopted, the received power $f(b_m)$ can be expressed as:

$$f(b_m) = \frac{\sigma_c^2}{3}\left[Q^{-1}\left(P_e/4\right)\right]^2\left(2^{b_i} - 1\right) \tag{33}$$

It can be seen the difference between QAM and MPSK is that the power allocated to each subcarrier is different when the number of bits is different. This paper takes MPSK as an example to verify the effectiveness of the improved greedy algorithm.

The complexity of greedy algorithm lies in the search sequence of each iteration. The improved greedy algorithm uses the bit step to allocate each bit, the number of iterations is approximately equal to the total number of the allocated bits $B = \sum_{m=1}^{N_c} b_m$. Table 2 gives the time complexity of the improved greedy algorithm and the optimal algorithm.

IV. SIMULATION AND ANALYSIS

In this section, the effectiveness of the proposed method is verified by simulation. Table 2 shows the OFDM shared waveform's parameters in the simulation, and the noise in the simulation is additive white Gaussian noise with zero mean. The computer is configured as CPU i7-8750h, and the Matlab version is R2016b.

A. BIT AND POWER ALLOCATION

The improved greedy algorithm is used to simulate the weighting optimal solution ($\omega_1 = \omega_2 = \omega_3 = 1/3$). The *SNR* of the OFDM shared waveform is 20 dB ($SNR = 10\lg p_T/\sigma_c^2$). It can be inferred from the objective function that with greater path propagation loss $\boldsymbol{\beta} = [\beta_1, \beta_2, \ldots, \beta_m], (m = 1, 2, \ldots, N_c)$, the channel gain

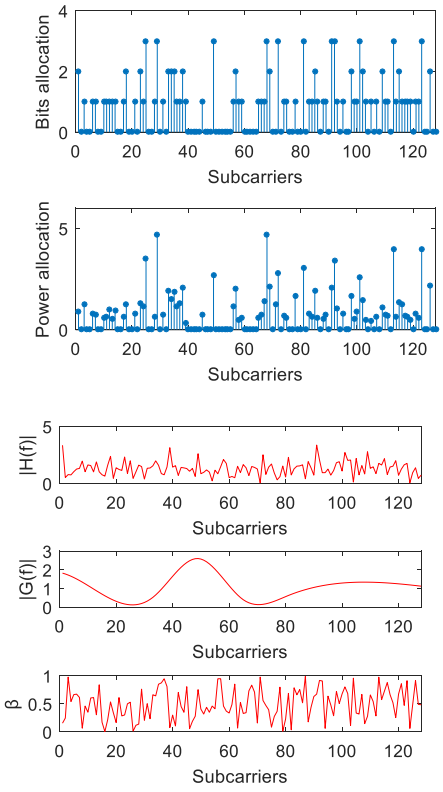

FIGURE 4. Power and bits allocation.

will be greater, and more power would be allocated on the corresponding subcarrier; with bigger $G(f)$, the clutter interference will be worse, and less power would be allocated on the corresponding subcarrier; with bigger $|H(f)|^2$, the communication channel's quality will be better, and more power would be allocated on the corresponding subcarrier.

From Figure 4, it can be seen that power allocation is the result of the trade-off among the radar, communication, and jamming performance under the combined effect of $\boldsymbol{\beta}$, $G(f)$, and $|H(f)|^2$. For example, on the 17^{th} subchannel, the path propagation loss gain is 0, and the corresponding subchannel does not allocate power and bits; on the 40^{th} to 60^{th} subcarriers, the radar channel has large clutter interference, and the allocation of power and bits is little; on the 124^{th} subcarrier, the communication channel has deep fading, and the allocated power and bits are zero, which shows the effectiveness of the algorithm.

Figure 5 shows the variation of the running time of the improved greedy algorithm and the optimal algorithm with the number of subcarriers. It can be seen that the running time of the two algorithms increases with the number of subcarriers, and the running time of the improved greedy algorithm is bigger than the optimal algorithm, because the optimal algorithm cannot achieve bit allocation, and the improved greedy algorithm discards part of the time complexity to achieve bit allocation. Simulation result shows that the improved greedy algorithm can achieve bit and power allocation with low time complexity.

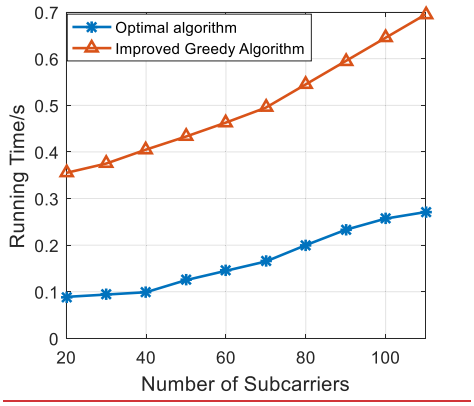

FIGURE 5. The variation of the running time with the number of subcarriers.

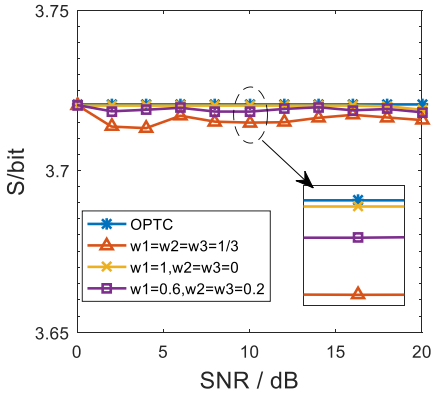

FIGURE 6. The variation of entropy with SNR.

B. PERFORMANCE ANALYSIS OF ADAPTIVE SHARED WAVEFORM

The frequency fading response of the communication channel $H(f)$ obeys Rayleigh distribution, the power spectral density of radar channel pulse response $G(f)$ is set as Gaussian process, and the propagation path loss $\boldsymbol{\beta} = [\beta_1, \beta_2, \ldots, \beta_m], (m = 1, 2, \ldots, N_c)$ obeys Gaussian distribution. The optimal suppressed jamming waveform given in Equation (7) is denoted as OPTS, the optimal radar waveform given in Equation (17) is denoted as OPTR, the optimal communication waveform given in Equation (20) is denoted as OPTC, and the weighting optimal waveform is represented by the weighting factors.

1) JAMMING PERFORMANCE

Figure 6 shows the variation of entropy with the SNR. Since the total power of transmission is constant, the jamming optimal curve obtained by (7) is a horizontal line, which can be regarded as the upper bound of entropy value. Comparing with the curves under different weighting factors obtained by the greedy algorithm, when the jamming weighting factor is equal to 1, the interference performance approaches the optimal upper bound. With the decrease of the jamming weighting factor, the entropy value is gradually reduced, that is to say, the suppression interference performance is gradually reduced.

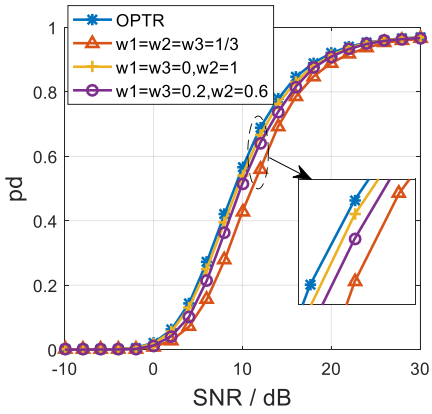

FIGURE 7. The variation of detection probability with SNR.

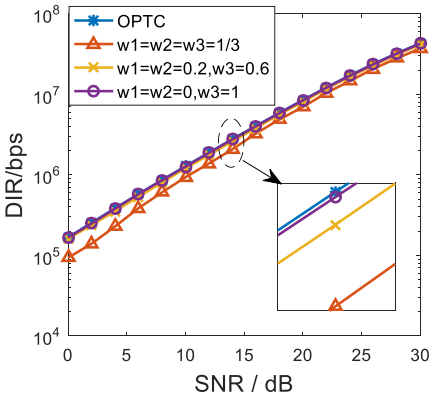

FIGURE 8. The variation of DIR with SNR.

2) RADAR PERFORMANCE

Figure 7 shows the variation of detection probability with SNR. The radar optimal curve obtained by (17) can be regarded as the upper bound of radar performance, but it cannot be achieved in practical application. Comparing the curves under different weighting factors obtained by the greedy algorithm, it can be seen that when the radar weighting factor is equal to 1, the radar performance differs by 2% compared with the optimal upper bound; with the increase of radar weighting factor, the detection probability gradually increases, that is, the radar detection performance gradually improves.

3) COMMUNICATION PERFORMANCE

Figure 8 shows the variation of DIR with SNR. The optimal communication curve obtained by (20) can be regarded as the upper bound of radar performance, but it cannot be achieved in practical application. Comparing the curves under different weighting factors obtained by the greedy algorithm, it can be seen that when the communication weighting factor is equal to 1, and the communication performance is 1% less than the optimal upper bound. With the increasing of communication weighting factor, the data information rate increases gradually, that is, the communication performance improves gradually.

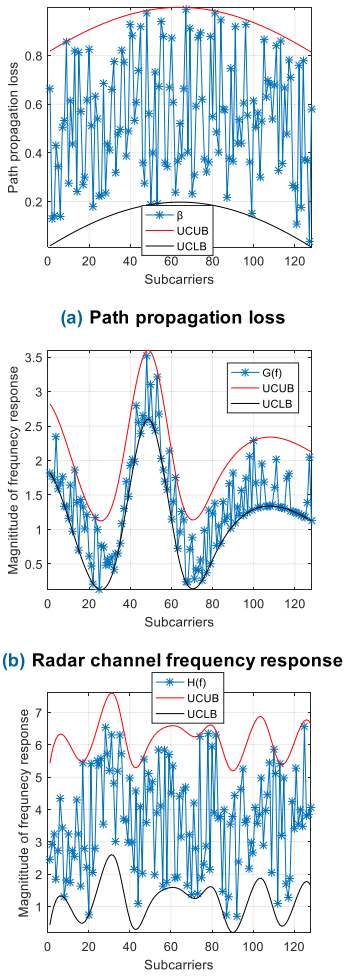

FIGURE 9. Path propagation loss and frequency response of radar and communication channel.

C. PERFORMANCE ANALYSIS OF ROBUST OFDM SHARED WAVEFORM

Fig. 9 shows the path propagation loss and radar and communication frequency response in the simulation. The optimal bit and power allocation scheme of (26) is given by the greedy algorithm. The waveform obtained by (26) is a robust waveform (RW), and the waveform obtained by (22) is non-robust waveform (NRW). When path propagation loss and frequency response of radar and communication channel are uncertainty class lower bound (UCLB), the following figures of the robust waveform and non-robust waveform are respectively expressed as "RW, AFR = UCLB " and "NRW, AFR = UCLB ". When path propagation loss and frequency response of radar communication channel are uncertainty class upper bound (UCUB), the following figures of the robust waveform and non-robust waveform are respectively expressed as "RW, AFR = UCUB" and "NRW, AFR = UCUB ". UCLB and UCUB are generated by "random" function in MATLAB.

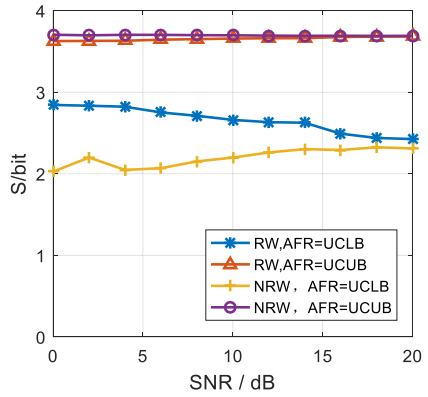

FIGURE 10. The variation of entropy with SNR.

1) JAMMING PERFORMANCE

Figure 10 shows the variation of entropy with SNR ($\omega_1 = \omega_2 = \omega_3 = 1/3$). When the path propagation loss and frequency response are lower bound of uncertainty class, the entropy of robust waveform is greater than the non-robust waveform, since the robust waveform is the best in the worst case of uncertainty class, and in the worst case, the performance of robust waveform is better than the non-robust waveform. When the path propagation loss and frequency response are upper bounds of the uncertainty class, the entropy of the robust waveform is not always greater than the non-robust waveform since the robust and non-robust waveforms are not optimal at this time. Under a certain SNR, the power of a waveform and the bit fraction formula is closer to the optimal distribution model. Therefore, the designed robust OFDM shared waveform improves the jamming performance in the worst case.

Figure 11 shows the variation of the entropy with the width of the uncertainty class ($\omega_1 = \omega_2 = \omega_3 = 1/3, SNR = 10dB$). From Figure 11 (a), it can be seen that when the real path propagation loss, and radar and communication frequency response are lower bound of the uncertainty class, the entropy of the robust and non-robust OFDM shared waveform is almost unchanged, since the lower bound of the uncertainty class is unchanged, and the performance of the robust shared waveform is always better than the non-robust OFDM shared waveform. When the real path transmission loss, and the radar and communication frequency response are upper bound of the uncertainty class, the interference entropy of the robust and non-robust OFDM shared waveforms increases with the increase of the uncertainty class, but at this time both of them are not optimal, and the entropy of the robust OFDM shared waveforms is not always larger than that of the non-robust OFDM shared waveforms.

From Figure 11 (b), it can be seen that when the real path transmission loss and radar communication frequency response are upper bound of the uncertainty class, the entropy of robust and non-robust waveforms is almost unchanged, since the upper bound of the uncertainty class is unchanged, and the entropy of the robust OFDM shared waveform is not always better than the non-robust OFDM shared waveform.

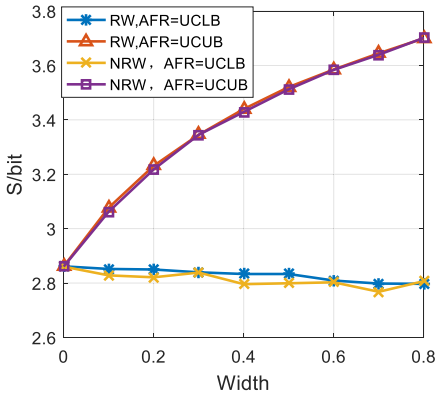

(a) The lower bounds are fixed

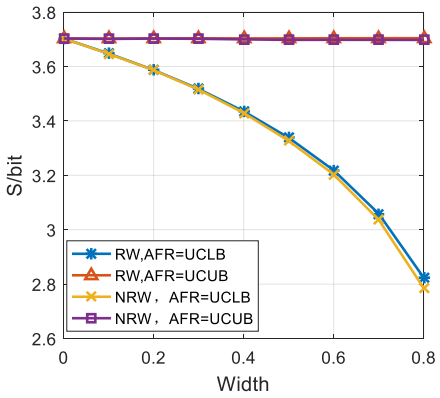

(b) The upper bounds are fixed

FIGURE 11. The variation of entropy with the width of uncertainty class.

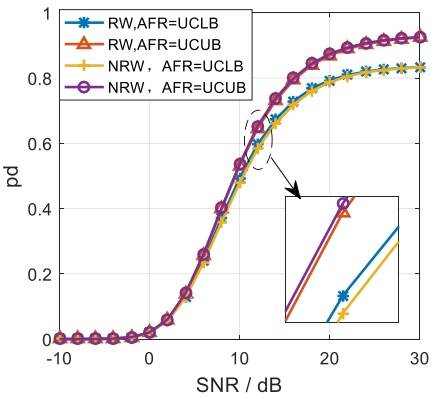

FIGURE 12. The variation of detection probability with SNR.

When the real path transmission loss and radar communication frequency response are lower bound of uncertainty class, the entropy of robust and non-robust OFDM shared waveform decreases with the increase of uncertainty class width, and the entropy of robust OFDM shared waveform is always greater than that of non-robust OFDM shared waveform.

2) RADAR PERFORMANCE

Figure 12 shows the variation of detection probability with SNR ($\omega_1 = \omega_2 = \omega_3 = 1/3$). From Figure 12, it can be seen that the detection probability increases with the increase of SNR. When the path propagation loss and frequency response

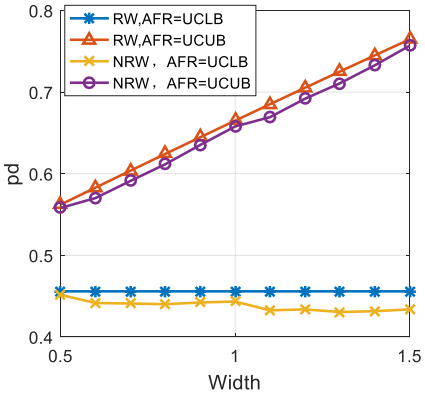

(a) The lower bounds are fixed

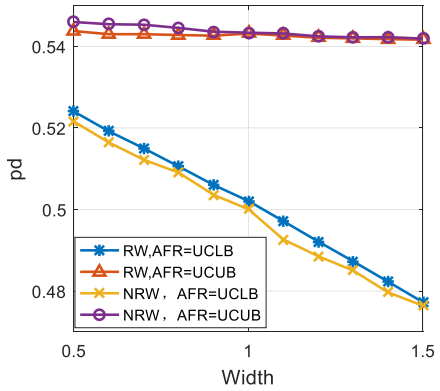

(b) The upper bounds are fixed

FIGURE 13. The variation of detection probability with the width of uncertainty class.

are the lower bound of uncertainty class, the detection probability of robust waveform is greater than the non-robust waveform, since the robust waveform is the optimal waveform in the worst case of uncertainty class, and in the worst case, the performance of robust waveform is greater than that of non-robust waveform. When the path propagation loss and frequency response are the upper bound of the uncertainty class, the detection probability of the robust waveform is not always better than that of the non-robust waveform, since the robust and non-robust waveform is not optimal at this time. With a certain SNR, the power and specific distribution of a waveform are closer to the optimal distribution. Therefore, the designed robust OFDM shared waveform improves the radar detection performance in the worst case.

Figure 13 shows the variation of detection probability with the width of the uncertainty class ($\omega_1 = \omega_2 = \omega_3 = 1/3, SNR = 10dB$). From Figure 13(a), it can be seen that when the real path propagation loss, and radar and communication frequency response are lower bound of the uncertainty class, the detection probability of the robust and non-robust OFDM shared waveform is almost unchanged, since the lower bound of the uncertainty set is unchanged, and the detection probability of the robust shared waveform is always larger than that of the non-robust OFDM shared waveform. When the real path transmission loss and the radar communication frequency response are the upper bound of

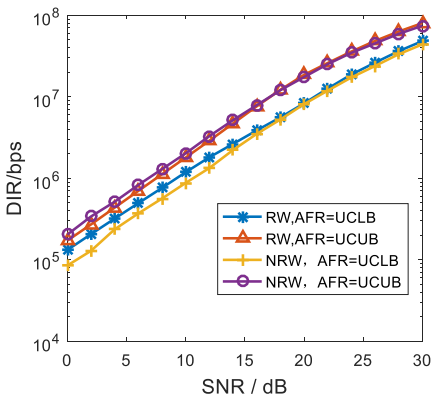

FIGURE 14. The variation of DIR with SNR.

the uncertainty class, the detection probability of the robust and non-robust shared waveform increases with the increase of the uncertainty class, but both of them are not optimal at this time.

From Figure 13(b), it can be seen that when the real path transmission loss, and radar and communication frequency response are upper bound of uncertainty class, the detection probability of robust and non-robust waveform is almost unchanged, since the upper bound of uncertainty set is unchanged. When the real path transmission loss, and radar and communication frequency response are lower bound of uncertainty class, the detection probability of robust and non-robust OFDM shared waveform decreases with the increase of uncertainty class width and the detection probability of robust OFDM shared waveform is always better than that of non-robust OFDM shared waveform.

3) COMMUNICATION PERFORMANCE

Figure 14 shows the variation of DIR with SNR ($\omega_1 = \omega_2 = \omega_3 = 1/3$). From Figure 14, it can be seen that the DIR increases with the increase of SNR. When the path propagation loss and frequency response are the lower bound of uncertainty class, the DIR of the robust waveform is better than the non-robust waveform, since the robust waveform is the best in the worst case of uncertainty class, and in the worst case, the performance of robust waveform is better than the non-robust waveform. When the path propagation loss and frequency response are upper bound of the uncertainty class, the DIR of the robust waveform is not always better than the non-robust waveform, since the robust and non-robust waveforms are not optimal at this time. Under a certain SNR, the power and bit allocation of a waveform is closer to the optimal allocation. Therefore, the designed robust OFDM shared waveform improves the communication performance in the worst case.

Figure 15 shows the variation of DIR with the width of the uncertainty class ($\omega_1 = \omega_2 = \omega_3 = 1/3, SNR = 10dB$). It can be seen from Figure 15(a) when the real path propagation loss, and radar and communication frequency response are lower bound of the uncertainty class, the DIR of the robust and non-robust OFDM shared waveforms is almost unchanged, because the lower bound of the

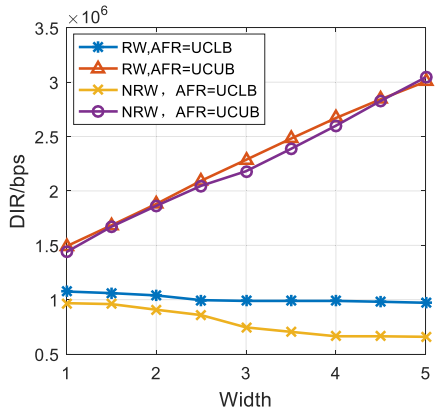

(a) The lower bounds are fixed

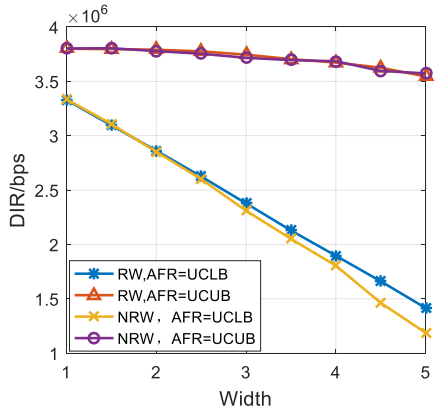

(b) The upper bounds are fixed

FIGURE 15. The variation of DIR with the width of uncertainty class.

uncertainty class is unchanged, and the DIR of the robust OFDM shared waveforms is always better than the non-robust OFDM shared waveforms. When the real path transmission loss, and the radar and communication frequency response are upper bound of the uncertainty class, the DIR of the robust and non-robust OFDM shared waveform increases with the increase of the uncertainty class. At this time, both of them are not optimal, and the DIR of the robust OFDM shared waveform is not always better than the non-robust OFDM shared waveform.

It can be seen from Figure 15(b) when the real path transmission loss, and radar and communication frequency response are upper bound of uncertainty class, the DIR of robust and non-robust waveforms is almost unchanged, because the upper bound of uncertainty set is unchanged, and the DIR of robust shared waveforms is not always better than the non-robust OFDM shared waveforms. When the real path transmission loss, and radar and communication frequency response are lower bound of uncertainty class, the DIR of robust and non-robust shared waveform decreases with the increase of uncertainty class width, and the DIR of the robust shared waveform is always better than the non-robust OFDM shared waveform.

V. CONCLUSION

In this paper, the optimization method of radar, communication, and jamming shared waveform based on OFDM is investigated. With the constraints of total power, an adaptive OFDM shared waveform and a robust OFDM shared waveform design method based on the improved greedy algorithm is given. In practical application, the performance of the OFDM integrated system can be adjusted by changing the weighting factor according to the radar detection, information transmission, and suppression interference requirements. Comparing with the performance of the non-robust OFDM shared waveform and the robust OFDM shared waveform, the robust OFDM shared waveform has acceptable performance in the whole uncertainty class. In the practical application of the OFDM integrated system, when the path propagation loss and radar communication frequency response are known, the non-robust shared waveform can be used, at this time, the performance of radar, communication, and jamming is optimal; when the path propagation loss and radar communication frequency response are unknown, the robust shared waveform can be used to ensure that the performance of radar, communication, and jamming has acceptable performance in the whole uncertainty class.

ACKNOWLEDGMENT

The author appreciate Prof. Ruijuan Yang for sharing her experience with me in OFDM shared waveform, and also Xiaobai Li, Jiajun Zuo, Dongjin Li, and Xitong Zhu who are all with Air Force Early Warning Academy for their technical assistance in the optimization thesis.

REFERENCES

[1] S. Sen, G. Tang, and A. Nehorai, "Multiobjective optimization of OFDM radar waveform for target detection," *IEEE Trans. Signal Process.*, vol. 59, no. 2, pp. 639–652, Feb. 2011, doi: 10.1109/TSP.2010.2089628.
[2] Y. Liu, Z. Yang, J. Xu, and G. Liao, "A super-resolution design method for integration of OFDM radar and communication," *J. Electron. Inf. Technol.*, vol. 38, no. 2, pp. 425–433, 2016.
[3] P. Kumari, J. Choi, N. Gonzalez-Prelcic, and R. W. Heath, Jr., "IEEE 802.11ad-based radar: An approach to joint vehicular communication-radar system," *IEEE Trans. Veh. Technol.*, vol. 67, no. 4, pp. 3012–3027, Apr. 2018, doi: 10.1109/TVT.2017.2774762.
[4] J. Moghaddasi and K. Wu, "Multifunctional transceiver for future radar sensing and radio communicating data-fusion platform," *IEEE Access*, vol. 4, pp. 818–838, 2016, doi: 10.1109/ACCESS.2016.2530979.
[5] A. Hassanien, M. G. Amin, Y. D. Zhang, and F. Ahmad, "Dual-function radar-communications: Information embedding using sidelobe control and waveform diversity," *IEEE Trans. Signal Process.*, vol. 64, no. 8, pp. 2168–2181, Apr. 2016, doi: 10.1109/TSP.2015.2505667.
[6] Y. Huang, B. Zhao, and M. Tao, "Review of synthetic aperture radar interference suppression," *J. Radars*, vol. 9, no. 1, pp. 86–106, 2020, doi: 10.12000/JR19113.
[7] D. Yu, Y. Wu, X. Jia, and Y. Wang, "Research on multiple phase sectional-ized modulation jamming method for pulse compression radar," *J. Signal Process.*, vol. 32, no. 10, pp. 1178–1186, 2016.
[8] Y. Liu, L. Zhang, S. Zhao, Q. Li, and J. Zhang, "Analysis and simulation of optimal deployment for netted radar under deception jamming," *J. Univ. Electron. Sci. Technol. China*, vol. 46, pp. 513–519, Apr. 2017.
[9] L. Lan, G. Liao, J. Xu, and Y. Zhang, "Main-beam range deceptive jamming suppression approach with FDA-MIMO radar," *Syst. Eng. Electron.*, vol. 40, no. 5, pp. 997–1003, May 2018.
[10] D. J. Bachmann, R. J. Evans, and B. Moran, "Game theoretic analysis of adaptive radar jamming," *IEEE Trans. Aerosp. Electron. Syst.*, vol. 47, no. 2, pp. 1081–1100, Apr. 2011, doi: 10.1109/TAES.2011.5751244.
[11] K. Huo and J. Zhao, "The development and prospect of the new OFDM radar," *J. Electron. Inf. Technol.*, vol. 37, no. 11, pp. 2776–2789, 2015.
[12] Y. Liu, G. Liao, J. Xu, Z. Yang, and Y. Zhang, "Adaptive OFDM integrated radar and communications waveform design based on information theory," *IEEE Commun. Lett.*, vol. 21, no. 10, pp. 2174–2177, Oct. 2017, doi: 10.1109/LCOMM.2017.2723890.

[13] Y. Liu, G. Liao, Z. Yang, and J. Xu, "Multiobjective optimal waveform design for OFDM integrated radar and communication systems," *Signal Process.*, vol. 141, pp. 331–342, Dec. 2017.
[14] C. Shi, F. Wang, M. Sellathurai, and J. Zhou, "Low probability of intercept based multicarrier radar jamming power allocation for joint radar and wireless communications systems," *IET Radar, Sonar Navigat.*, vol. 11, no. 5, pp. 802–811, May 2017, doi: 10.1049/iet-rsn.2016.0362.
[15] S. Yin and Z. Qu, "Resource allocation in multiuser OFDM systems with wireless information and power transfer," *IEEE Commun. Lett.*, vol. 20, no. 3, pp. 594–597, Mar. 2016, doi: 10.1109/LCOMM.2016.2516999.
[16] A. Aubry, A. De Maio, M. Piezzo, and A. Farina, "Radar waveform design in a spectrally crowded environment via nonconvex quadratic optimization," *IEEE Trans. Aerosp. Electron. Syst.*, vol. 50, no. 2, pp. 1138–1152, Apr. 2014, doi: 10.1109/TAES.2014.120731.
[17] Y. Chen, Y. Nijsure, C. Yuen, Y. H. Chew, Z. Ding, and S. Boussakta, "Adaptive distributed MIMO radar waveform optimization based on mutual information," *IEEE Trans. Aerosp. Electron. Syst.*, vol. 49, no. 2, pp. 1374–1385, Apr. 2013, doi: 10.1109/TAES.2013.6494422.
[18] D. Ciuonzo, A. De Maio, G. Foglia, and M. Piezzo, "Intrapulse radar-embedded communications via multiobjective optimization," *IEEE Trans. Aerosp. Electron. Syst.*, vol. 51, no. 4, pp. 2960–2974, Oct. 2015, doi: 10.1109/TAES.2015.140821.
[19] C. Shi, F. Wang, M. Sellathurai, J. Zhou, and S. Salous, "Power minimization-based robust OFDM radar waveform design for radar and communication systems in coexistence," *IEEE Trans. Signal Process.*, vol. 66, no. 5, pp. 1316–1330, Mar. 2018, doi: 10.1109/TSP.2017.2770086.
[20] Y. Liu, "Transmit power adaptation for orthogonal frequency division multiplexing integrated radar and communication systems," *J. Appl. Remote Sens.*, vol. 11, no. 3, p. 1, Sep. 2017.
[21] G. Wang, J. Bai, D. Sun, and X. Zhang, "A suppression algorithm of blanket-distance deception compound jamming based on joint signal-data processing," *J. Electron. Inf. Technol.*, vol. 40, no. 10, pp. 2430–2437, 2018, doi: 10.1109/TSP.2017.2770086.
[22] J. Zuo, R. Yang, S. Luo, and X. Li, "Training sequence design of TDS-OFDM signal in joint radar and communication system," *Math. Problems Eng.*, vol. 2019, pp. 1–10, Jul. 2019.
[23] S. Garrido-Jurado, R. Muñoz-Salinas, F. J. Madrid-Cuevas, and R. Medina-Carnicer, "Generation of fiducial marker dictionaries using mixed integer linear programming," *Pattern Recognit.*, vol. 51, pp. 481–491, Mar. 2016.
[24] S. Kay, "Optimal signal design for detection of Gaussian point targets in stationary Gaussian Clutter/Reverberation," *IEEE J. Sel. Topics Signal Process.*, vol. 1, no. 1, pp. 31–41, Jun. 2007, doi: 10.1109/JSTSP.2007.897046.
[25] D. Steven and S. Boyd, "CVXPY: A Python-embedded modeling language for convex optimization," *J. Mach. Learn. Res.*, vol. 17, no. 1, pp. 2909–2913, 2016.
[26] Z. Ren, S. Chen, B. Hu, and W. Ma, "Proportional resource allocation with subcarrier grouping in OFDM wireless systems," *IEEE Commun. Lett.*, vol. 17, no. 5, pp. 868–871, May 2013, doi: 10.1109/LCOMM.2013.031913.122706.
[27] D. P. Palomar and J. R. Fonollosa, "Practical algorithms for a family of waterfilling solutions," *IEEE Trans. Signal Process.*, vol. 53, no. 2, pp. 686–695, Feb. 2005, doi: 10.1109/TSP.2004.840816.
[28] Y. Huang, Y. He, Q. Luo, L. Shi, and Y. Wu, "Channel estimation in MIMO–OFDM systems based on a new adaptive greedy algorithm," *IEEE Wireless Commun. Lett.*, vol. 8, no. 1, pp. 29–32, Feb. 2019, doi: 10.1109/LWC.2018.2848916.
[29] K. El Baamrani, V. P. G. Jimenez, A. G. Armada, and A. A. Ouahman, "Multiuser subcarrier and power allocation algorithm for OFDM/offset-QAM," *IEEE Signal Process. Lett.*, vol. 17, no. 2, pp. 161–164, Feb. 2010, doi: 10.1109/LSP.2009.2035380.

SHENGKUN ZHU was born in Jiamusi, China, in 1996. He received the B.S. degree in information and communication engineering from the Dalian University of Technology, Dalian, China, in 2018. He is currently pursuing the M.S. degree with the Air Force Early Warning Academy, Wuhan, China. His current research interests include radar signal processing, radar waveform design, and intelligent application of integrated systems.

RUIJUAN YANG was born in Zhongjiang, China, in 1964. She received the B.S. and M.S. degrees from the Chengdu University of Electronic Science and Technology, China, in 1984 and 1987, respectively, and the Ph.D. degree from the Huazhong University of Science and Technology, Wuhan, China. She is currently a Professor with the Air Force Early Warning Academy, Wuhan. She is a high-level airforce talent and an air force-level expert. She has completed more than 20 scienti_c major research projects both inside and outside the military. She has authored more than 60 articles. She holds four patents. She has been granted one software copyright. Her research interests include communication technology, radar signal processing, integrated radar communication technology, machine learning, and intelligent application of integrated systems. She received seven military science and technology talent progress awards.

XIAOBAI LI was born in Longxi, China, in 1983. He received the B.S., M.S., and Ph.D. degrees from the Radar Academy, Wuhan, China, in 2006, 2009, and 2013, respectively. He is currently a Lecturer with the Laboratory of Radar and Communication Integrated Technology, Air Force Early Warning Academy. His current research interests include integrated radar communication technology, machine learning, radar signal processing, and waveform design and optimization.

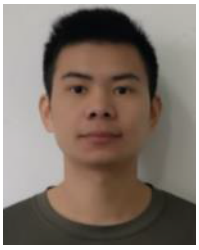

JIAJUN ZUO was born in Wuhan, China, in 1992. He received the B.S. and M.S. degrees from the Air Force Early Warning Academy, Wuhan, in 2013 and 2016, respectively, where he is currently pursuing the Ph.D. degree in information and communication engineering. His research interests include radar signal processing, radar waveform design, and intelligent application of integrated systems.

DONGJIN LI was born in Guangyuan, China, in 1992. He received the B.S. and M.S. degrees from the Air Force Early Warning Academy, Wuhan, China, in 2014 and 2017, respectively, where he is currently pursuing the Ph.D. degree in information and communication engineering. His research interests include deep learning, dictionary learning, radar signal processing, machine learning, and intelligent application of integrated systems.

YATING DING was born in Suzhou, China, in 1996. She received the B.S. degree in social work from Anhui University, Hefei, China, in 2019. She is currently pursuing the M.S. degree with Wuhan University, Wuhan, China. Her current research interests include natural language process and depression.